

Prestack $v(z)$ f-k migration from common-offset sections

Xinxiang Li and Gary F. Margrave

ABSTRACT

A scheme of migration from separated common-offset sections using the $v(z)$ f-k nonstationary filtering theory is presented in this paper. It is a direct extension of the $v(z)$ f-k CDP-offset domain prestack migration algorithm for the whole prestack data volume. This migration scheme provides high quality migration images and opportunities for migration error correction, especially for converted wave data migration where migration velocities are difficult to observe. The current computer implementation of the algorithm is accurate but very time consuming. Along with the migration algorithm, partial NMO required by common-offset binning before NMO correction is also discussed.

INTRODUCTION

Migration from separated common-offset sections has been a theoretical and practical issue in seismic data processing since the 1970's. Publications, such as Gardner et al. (1974), Sattlegger et al. (1980) and Deregowski (1990), discussed the methods of migration velocity analysis using the migration results of separated offset sections. Some recent papers, such as Kim and Krebs (1993), gave more detailed and careful discussion on the practical application of these methods. Kim and Krebs (1993) also showed some examples of stacking migrated offset sections, and they suggest that migration velocities and the stacking velocities for stacking migrated offset sections may need more than one iteration to improve the final image. Recent developments in migration theory and related amplitude issues demand the necessity of obtaining migrated common-offset sections as images of the subsurface (rather than just a tool for providing one final image). These migrated sections theoretically provide more reliable offset-dependent reflection coefficients for AVO or AVA analysis although AVO analysis directly from CMP gathers has been quite successful.

Diffraction-summation type migration methods have been used for migration of common-offset sections for decades, and they have been successful for migration velocity analysis because their efficiency and independence from acquisition geometry. However, when more accurate amplitude consideration is required, Fourier domain methods, such as the phase-shift migration, are preferred. Many publications have discussed the numerical and practical feasibility of the phase-shift method to migrate common-offset sections. Popovici (1994) presented a method of produce migrated offset sections by the direct decomposition of the double-square-root (DSR) based prestack phase-shift algorithm in the CDP-offset domain. Alkhalifah (1997) presented a similar phase-shift time migration from offset sections for transversely isotropic media with vertical symmetry axis (VTI). Ekren and Ursin (1995, 1999) presented a prestack time migration through some simplification of the offset-section phase-shift migration scheme developed by Dubrulle (1983). Etgen (1998) and Rietveld et al (1998) found that, when the velocity has only vertical variation, migration of common-offset common-azimuth data volume can be very efficient with the computation advantage of the multi-dimensional Fourier transform. Dai and

Marcoux (1999) also discussed common-offset and common-azimuth migration scheme with their own implementation strategies. Jin and Wu (1999) started from the time-space domain DSR equation and developed an offset-section depth migration algorithm using the generalized screen propagation (GSP) concept, which can accommodate lateral velocity variation.

As for the applications of common-offset section migration to AVO analysis, Ekren and Ursin (1995, 1999) showed some examples with their migration algorithm and some additional careful amplitude considerations. AVO or AVA analysis after migration is a topic drawing more and more attentions (Mosher et al., 1996, Tygel et al., 1999).

This paper presents the $v(z)$ f-k scheme for common-offset migration as a nonstationary filtering (Margrave, 1998a) process. Compared with migration directly from the full prestack data volume, it is mainly a different way to compute the nonstationary migration filters. This scheme contains a main loop over wavenumbers in the CDP direction, instead of a loop over depth steps in conventional phase-shift algorithms. The $v(z)$ f-k algorithm is an analogue of Stolt's f-k migration with convenient accommodation of vertical velocity variation. The formulations and discussions in this paper are all based on the assumption that the migration velocities only change in depth.

FROM FULL PRESTACK MIGRATION TO COMMON-OFFSET SECTION MIGRATION

Wavefield extrapolation can be explicitly expressed in the Fourier domain using the DSR equation in the CDP-offset domain. If k_x and k_h represent the wavenumbers in CDP and offset direction, and ω represents the temporal frequency, the wavefield at any depth z can be directly obtained from the wavefield at depth 0 , which is an approximate representation of the seismic wavefield recorded at the earth's surface. After Li and Margrave (1998), the extrapolation process can be written as

$$\begin{aligned} & \psi(k_x, k_h, z, \omega) \\ &= \psi(k_x, k_h, 0, \omega) \exp \left(-i \int_0^z \left[\sqrt{\frac{\omega^2}{v_S^2(z')} - \left(\frac{k_x - k_h}{2}\right)^2} + \sqrt{\frac{\omega^2}{v_R^2(z')} - \left(\frac{k_x + k_h}{2}\right)^2} \right] dz' \right) \quad (1) \\ &= \psi(k_x, k_h, 0, \omega) \cdot m(k_x, k_h, z, \omega), \end{aligned}$$

where v_S and v_R are velocities for downgoing (S stands for source) and upcoming waves (R stands for receiver). The migration result (image), which is represented by the wavefield at time $t=0$ and offset $h=0$, can then be expressed as

$$\begin{aligned} \Psi(x, 0, z, 0) &= \iiint \psi(k_x, k_h, z, \omega) \exp(-ik_x x) dk_x dk_h d\omega \\ &= \iiint \psi(k_x, k_h, 0, \omega) \cdot m(k_x, k_h, z, \omega) \exp(-ik_x x) dk_x dk_h d\omega. \quad (2) \end{aligned}$$

If the input data contains only one offset section, it is not straightforward to consider it as a wavefield. A convenient way to still use the wavefield concept is to assume that all other offset sections are present but with zero amplitudes. Using the

delta-function notation, the input data containing only the traces with a constant offset value h_0 can be expressed as

$$\Psi_{h_0}(x, h, 0, t) = \Psi(x, h, 0, t) \delta(h - h_0), \quad (3a)$$

and its 2D Fourier transform over x and t can be expressed as

$$\varphi_{h_0}(k_x, h, 0, \omega) = \varphi(k_x, h, 0, \omega) \delta(h - h_0). \quad (3b)$$

Therefore the 3-D Fourier transform of such a wavefield is

$$\psi(k_x, k_h, 0, \omega) = \int \varphi_{h_0}(k_x, h, 0, \omega) e^{ik_h h} dh = \varphi(k_x, h_0, 0, \omega) e^{ik_h h_0}. \quad (4)$$

Substitute (4) into (2) so that the image can be expressed as

$$\Psi(x, 0, z, 0) = \iiint \varphi(k_x, h_0, 0, \omega) e^{ik_h h_0} m(k_x, k_h, z, \omega) \exp(-ik_x x) dk_x dk_h d\omega. \quad (5)$$

The integral over the offset-wavenumber, k_h , can be isolated and combined into the migration filter term, m in equations (1) and (2). Therefore a new migration filter m_{h_0} is introduced as

$$m_{h_0} = \int m(k_x, k_h, z, \omega) e^{ik_h h_0} dk_h. \quad (6)$$

The image from a single offset section then becomes

$$\Psi(x, 0, z, 0) = \iint \varphi(k_x, h_0, 0, \omega) m_{h_0}(k_x, z, \omega) \exp(-ik_x x) dk_x d\omega. \quad (7)$$

These offset-specific migration filters are matrix functions of given k_x and ω , and require an integral over offset wavenumbers, k_h . Careful selection of k_h sampling is required because insufficient sampling may cause serious wrap-around effects (aliasing) in the offset direction. Popovici (1994) presented an adaptive sampling of offset-wavenumbers in certain limits to overcome this problem. The main point is to assume enough offset range even though only one offset section is involved in the migration scheme.

The computation of the migration filters expressed in equation (6) takes almost the same amount of time as the computation of the migration filters for migrating the whole prestack data volume because of the integral over assumed offset-wavenumbers. Many authors use approximate methods (such as stationary-phase method) to evaluate the k_h -integrals (Popovici, 1994, Alkhalifah, 1997, Dai and Marcoux, 1999). The stationary-phase method and the trapezoidal Filon method for the approximations to such integrals are discussed in Li and Margrave (1999b).

The results shown later in this paper were obtained from the accurate (but very slow) algorithm, which is implemented directly using equations (6) and (7).

COMMON-OFFSET BINNING AND PARTIAL NMO

Common-offset sections should be formed before NMO correction for the purpose of prestack migration. Unlike offset binning for DMO processing, where the data are usually NMO corrected, offset binning before NMO may involve traveltimе corrections at each offset bin center. This local moveout correction (includes NMO and inverse NMO) is called partial NMO correction. If the bin width of an offset section is not large, the traveltimе differences on different traces in one offset bin may not be a serious problem, but small traveltimе differences might still result in lower resolution (narrower frequency band) on the binned traces.

Large offset bin-size could be an efficient way to lower the cost of the offset-section migration process, but the accuracy of the partial NMO velocity should be considered. In Figure 1, two common-offset sections centered at zero-offset with a bin-width equal to 300 m are shown, where (a) is the section without any partial NMO applied and (b) is the section partially NMO corrected using the available stacking velocities. The quality of section (b) is better than the one in (a), especially the events at the earlier times.

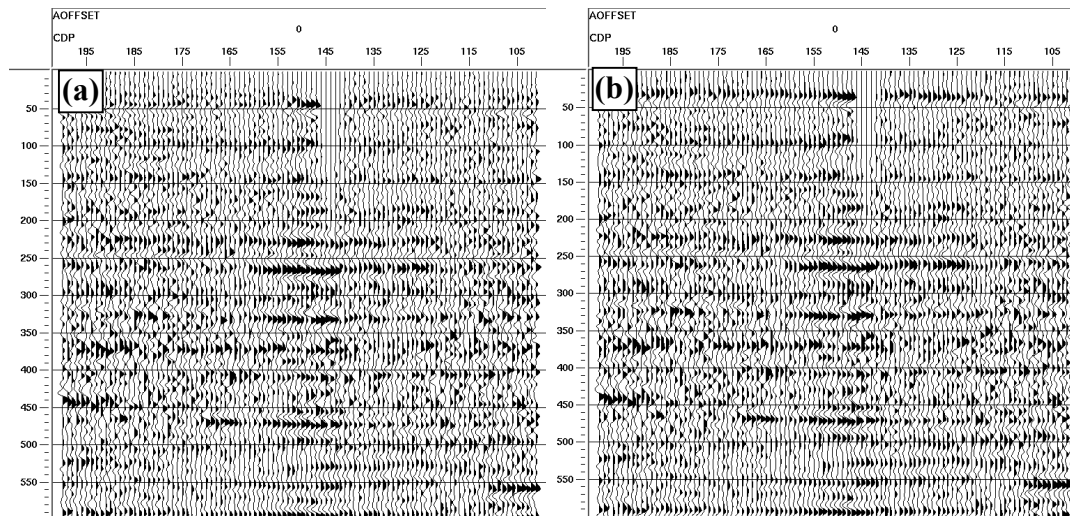


Figure 1: Common-offset sections with its center at zero-offset and bin-width equal to 300 meters, where (a) without partial NMO and (b) with partial NMO with stacking velocity.

The differences between Figure 1(a) and Figure 1(b) are not very obvious because the very near offset (-150 m to 150 m in the examples) traces do not have significant moveout differences. More serious problem occurs when common-offset binning is performed for traces with relatively large offsets. Figure 2 shows two sections both centered at offset 1200 m and with the same bin-width of 300 m, where (a) is the section without partial NMO correction, and (b) is the section with partial NMO correction using stacking velocity. Many events that appear clearly on section (b) virtually disappeared on section (a). The detail features of the target (from CDP 130 to 170 and below 1100 ms in the display) clearly seen in (b) are also badly blurred in (a).

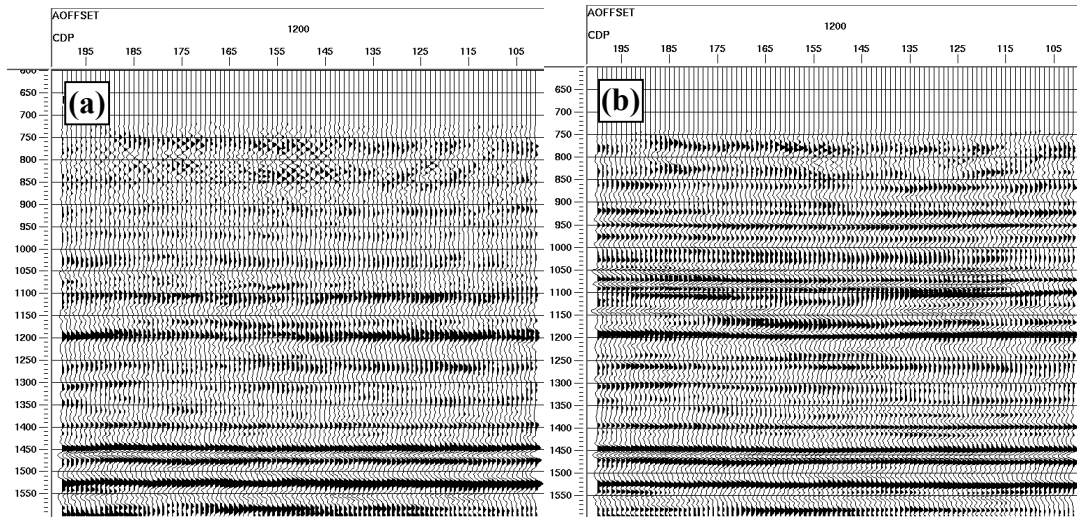


Figure 2: Common-offset sections centered at offset equal to 1200 m and with bin-width equal to 300 meters, where (a) without partial NMO and (b) with partial NMO with stacking velocity.

MIGRATION RESULTS FROM BLACKFOOT PP DATA

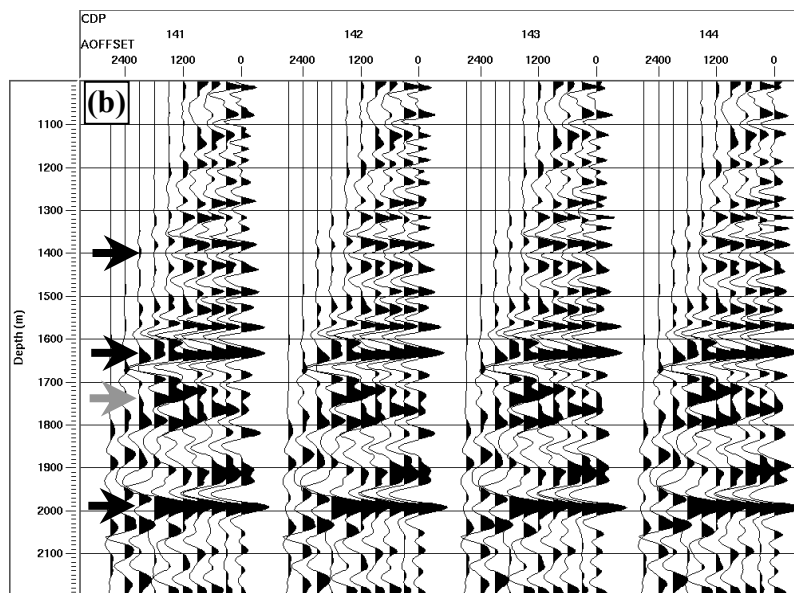
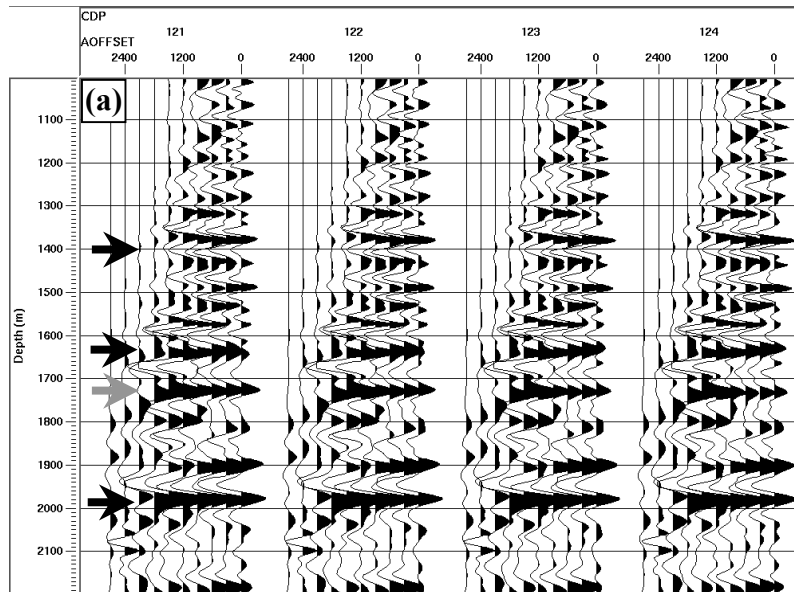
The current computer implementation of the $v(z)$ f - k common-offset-section migration algorithm presented in this paper has been completed as a module in ProMAX 2D. Although the computation of the migration process is time consuming, the results obtained are informative. Some results are presented using the Blackfoot III 2D vertical and radial-component data.

The vertical-component data was first binned into common-offset sections with center-offset values ranging from 0 to 2700 m with an increment of 300 m. Partial NMO corrections were applied with the available stacking-velocity field. The migration velocity was the P-wave depth-interval velocity converted from the stacking velocity.

Figure 3 shows four groups of common-image gathers (A common-image gather gathers all migrated traces at one given CDP location). As the notations in the figures indicated, (a) shows 4 image gathers at CDPs 121, 122, 123, and 124; (b) shows 4 image gathers at CDPs 141, 142, 143, and 144; (c) shows 4 image gathers at CDPs 161, 162, 163, and 164; and (d) shows 4 image gathers at CDPs 181, 182, 183, and 184. The target of this dataset is a sand-channel located between CDP numbers 130 and 170. The four groups of gathers start from west outside (corresponding to smaller CDP numbers) of the sand-channel and extend to the east outside of the channel. The displays are all windowed in depth from 1000 m to 2200 m. The target depth on these image gathers is between 1700 m and 1900 m. [This depth is about 200 meters deeper than the geological target depth, and this mismatch is discussed in Li and Margrave (1998) and Li et al. (1999).]

The following observations can be obtained from these common-image gathers:

- The events on the gathers are quite flat, and this implies that the velocity field used for migration is quite accurate.
- Some major events, such as the ones indicated by small **black-coloured** arrows, do not have significant changes at different CDP locations cross the sand-channel area.
- As indicated by **grey-coloured** arrows, the event (corresponding to Mississippian) very well focused at CDP locations 121 to 124 (outside west of the sand-channel) becomes blurred at CDP locations 141 to 144 (inside the sand-channel), but reappears focused at CDP locations 181 to 184, which are located outside east of the sand-channel.



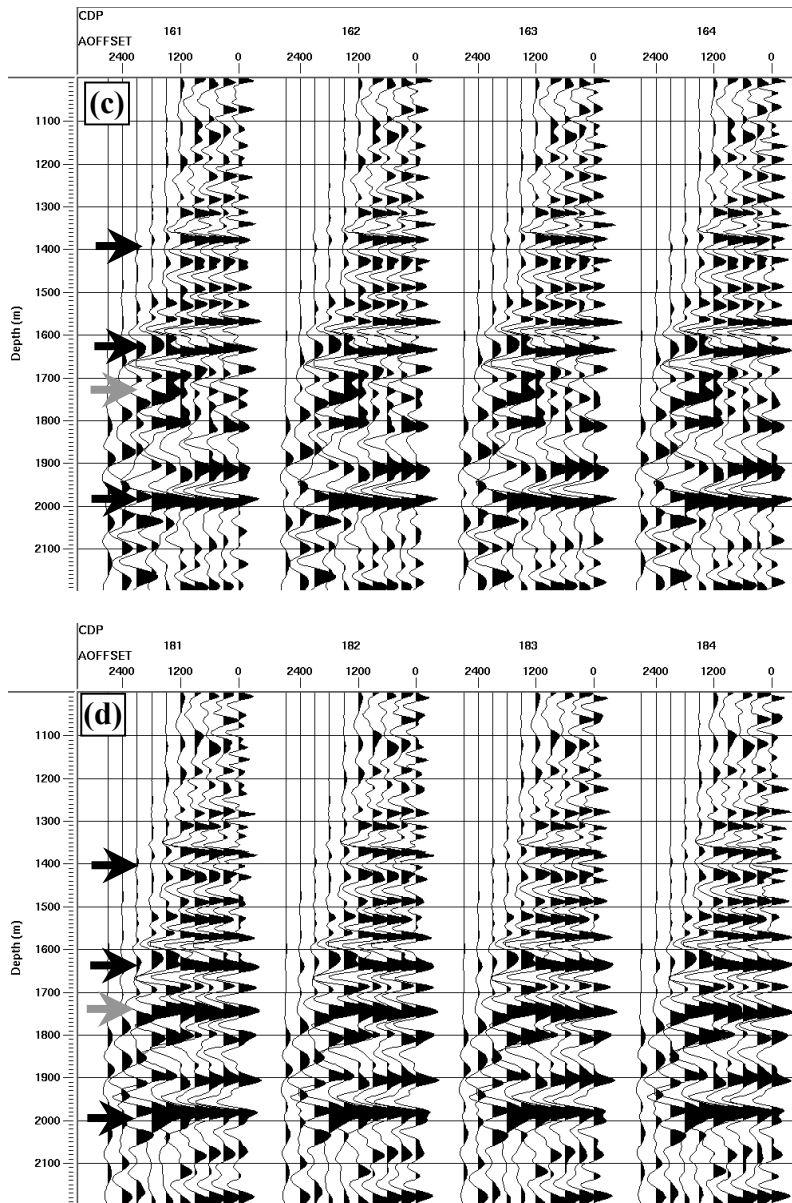


Figure 3: Common-image gathers at 16 different CDP locations in 4 group, where (a) shows 4 image gathers at CDP 121 to 124, (b) shows 4 gathers at CDP 141 to 144, (c) shows gathers at CDP 161 to 164, and (d) shows 4 gathers at CDP 181 to 184.

Figure 4 shows some comparisons between CMP gathers and the migrated common-image gathers at the same CDP location (CDP number 122). (a) shows the common-offset binned CMP gather with a bin-width of 100 m, (b) shows the common-offset binned gather with a bin-width of 300 m. As expected, the gather in (a) provides more detailed information of the reflection events, and (b), however, has higher signal-to-noise ratio. Most of the features in (a) are still recognisable in (b). Figure 4(c) shows the common-image gathers at the same CDP location. This gather is displayed in two-way zero-offset time. There are some differences between the gather before migration (b) and after migration (c), however, not many conclusions can be drawn before more detailed analysis.

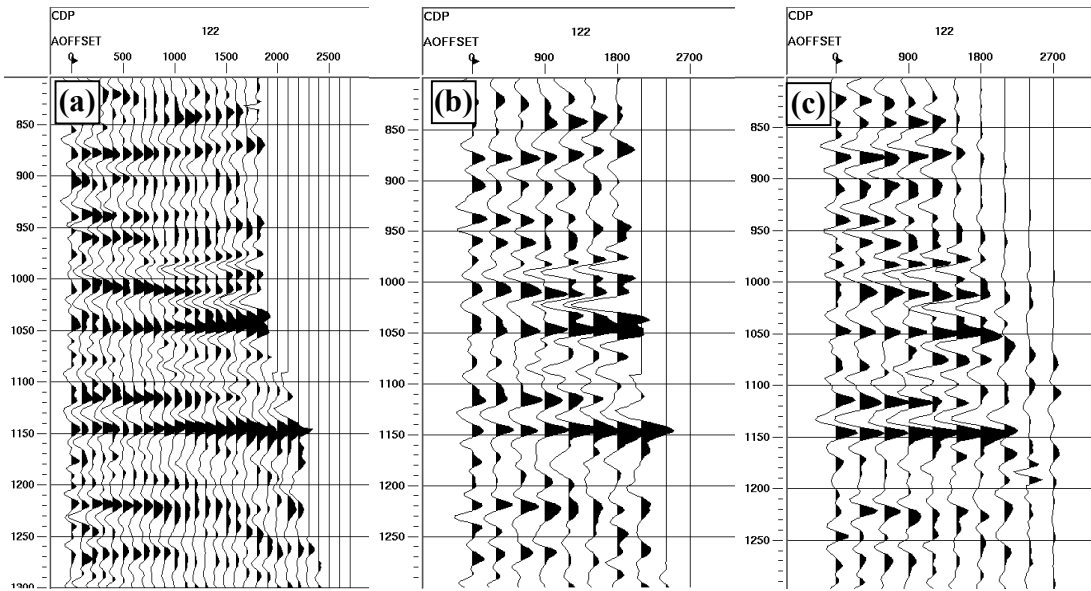


Figure 4: NMO corrected CMP gather after common-offset binning with (a) small bin-width of 100 m and (b) larger bin range of 300 m. (c) is the migrated common-image gather at the same CMP location from larger bin-range offset-binned data.

The comparison between the stacked image from all migrated common-offset sections and the image migrated directly from the full prestack volume may also reveal necessity of migration from separated common-offset sections. Figure 5 shows a portion of the image of the Blackfoot vertical-component data obtained by stacking all the migrated offset sections, and Figure 6 shows the same portion of the image obtained by directly migrating from the prestack data volume. The image in Figure 5 has higher resolution (and it is difficult to explain why).

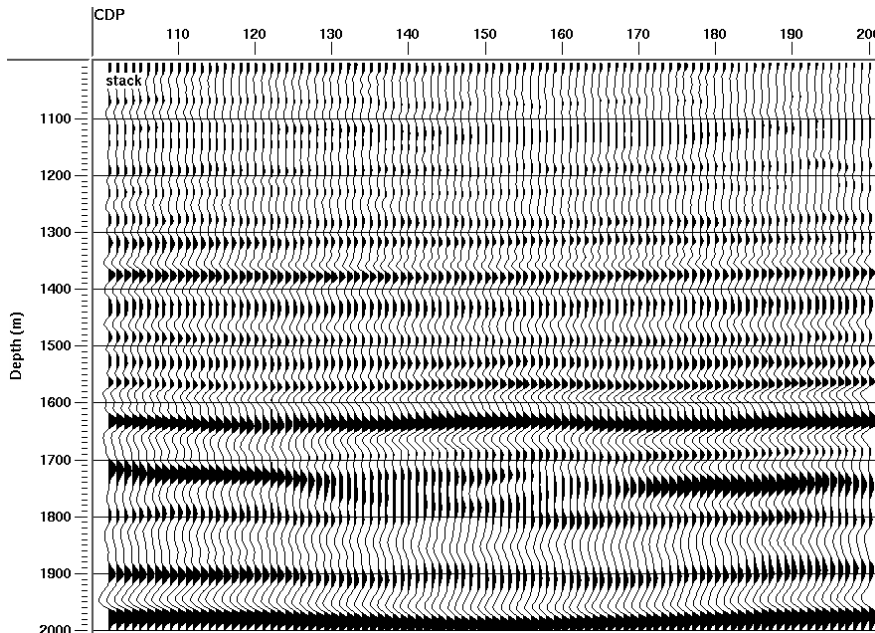


Figure 5: A portion of the PP image of the Blackfoot vertical-component data obtained by stacking all the migrated offset sections.

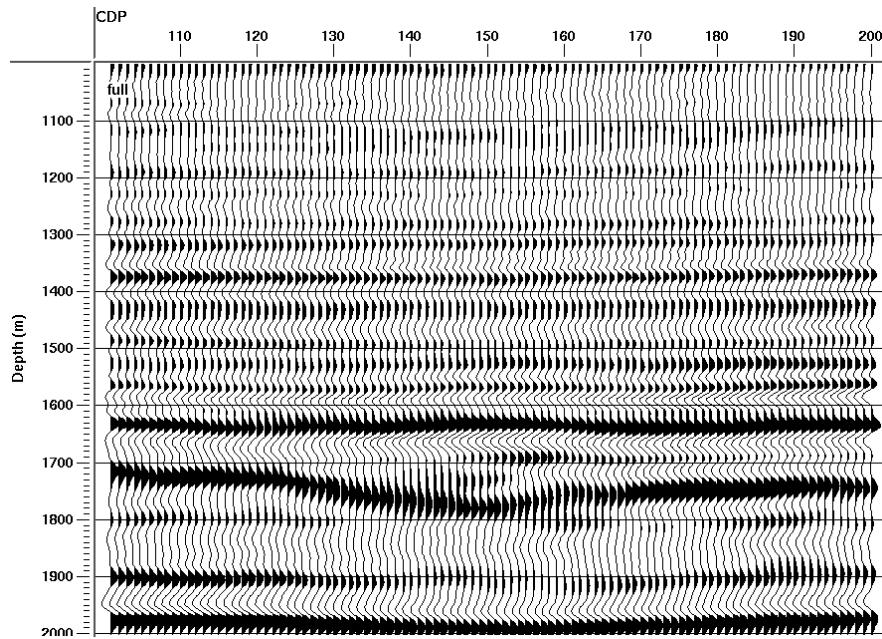


Figure 6: A portion (same location as the one shown in Figure 5) of the image obtained by directly migrating from the prestack whole volume.

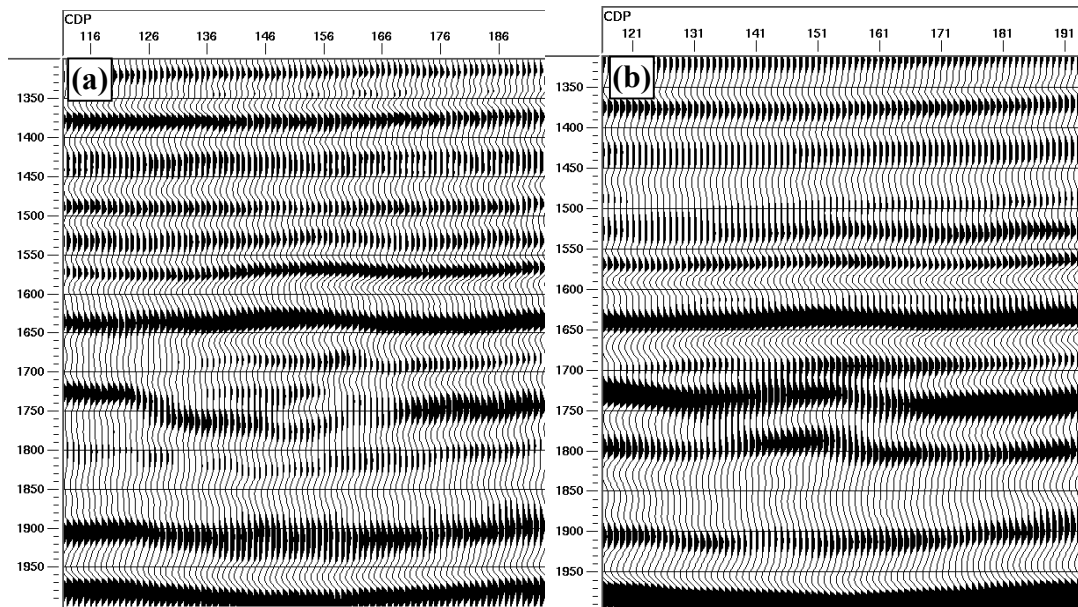


Figure 7: Target sand-channel images (a) from stacking near offset (range from 0 to 1350 m) migrated common-offset sections and (b) from stacking middle-range offset (range from 1050 to 2250 m) migrated common-offset sections.

As separate images for the same subsurface, migrated common-offset sections provide more information (such as offset dependence) than the only one image directly obtained from the whole data volume. Figure 7 shows two stacked images from the migrated common-offset sections, where (a) is the image stacked from the migrated common-offset sections with absolute-offsets from 0 to 1350 m, and (b) is the image stacked from the migrated common-offset sections whose absolute-offsets

range from 1050 to 2250 m. It can be seen that section in (a) has higher resolution. More detailed analysis is needed to obtain meaningful interpretations, such as AVO anomalies.

SOME RESULTS FROM BLACKFOOT RADIAL-COMPONENT DATA

The $v(z)$ f-k migration algorithm can be easily implemented to migrate converted wave data before common conversion point (CCP) binning (Li and Margrave, 1998). The CCP binning process is included in the migration algorithm. This is feasible because the accurate velocity information, as a requirement for the migration process, ensures accurate depth-variant CCP binning.

The migration of the Blackfoot radial-component data used the P-wave depth-interval velocity converted from the best stacking velocity for the vertical-component data, and the S-wave depth-interval velocity computed from shear wave well-log information. The radial-component data are common-offset binned with offset-bin-centres at -2700 to 2700 m with 300 m bin-width. The offset-binning partial-NMO velocities were directly picked from the CMP gather before binning. The resultant binned data contained a total of 19 common-offset sections, and its migration took more than twice the computation time used to migrate the vertical-component data because the migration filters for converted waves data cost more computations (in addition to the almost twice number of offset sections).

Figure 8 shows four consecutive common-image gathers at CDP 161 to 164. Unlike the results from the vertical-component data discussed previously, many events in the gathers are not flat. This implies that the migration velocity field used was not accurate. Directly stacking common-image gathers like the ones shown in Figure 8 will significantly reduce the resolution of the image section, and may even destroy some events.

One advantage of migrating common-offset sections separately is that the migration velocity can be assessed for accuracy before stacking the migration results. It is fortunate that the migration of one common-offset section is not very sensitive to the migration velocity errors (Ferber, 1994, Kim and Krebs, 1993, and Deregowski, 1990). A widely used method for velocity-error correction for common-offset migration gathers is to inverse-NMO correct the migrated data, and perform a conventional velocity analysis and finally NMO correct and stack the common-image gathers.

Figure 9 shows four common-image gathers at the same locations as the four gathers shown in Figure 8. The new gathers have been well flattened by the inverse NMO and re-NMO with a new velocity field. Stacking common-image gathers as in Figure 9 will result in better image than stacking the gathers in Figure 8. Sometimes, another iteration of forming common-image gathers may be needed.

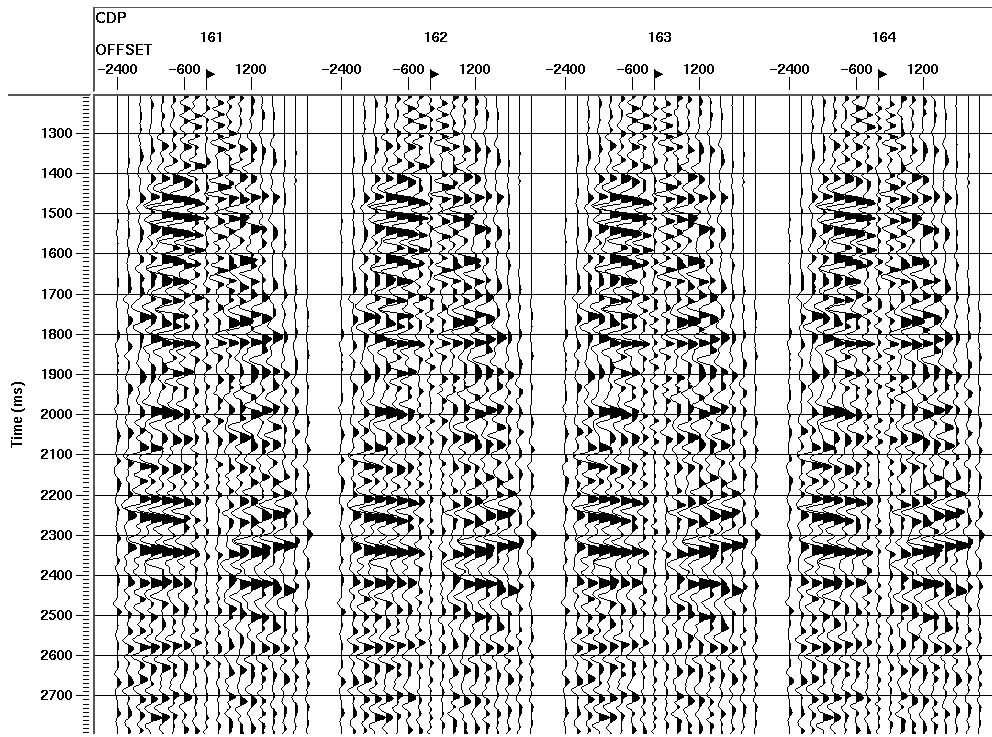


Figure 8: Common-image gathers migrated from radial component common-offset sections using the $v(z)$ f-k algorithm.

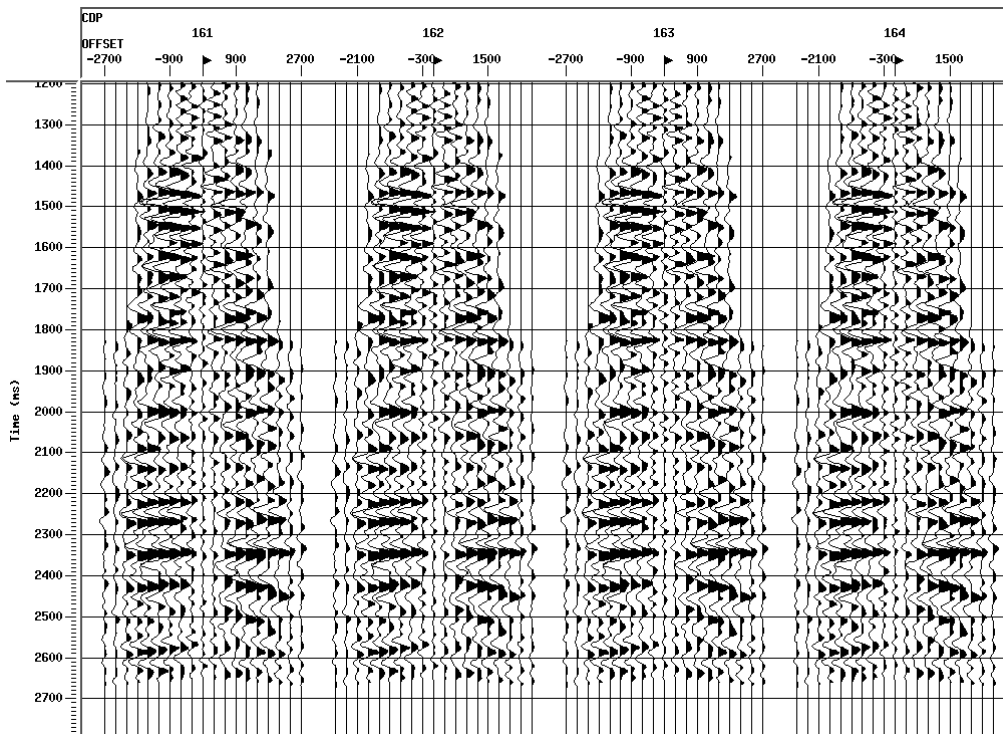


Figure 9: Common-image gathers after INMO with the CMP NMO velocity and then NMO correction with a re-picked velocity.

The inverse NMO correction in the above error-correction process used the velocity picked on radial-component CMP gathers before binning. This velocity can be picked because the reflection moveout on the CMP gathers of radial-component data is still approximately hyperbolic, and the accuracy of this velocity is not a major concern in this process.

As discussed in Li and Margrave (1998, 1999a), the $v(z)$ f-k prestack converted wave migration algorithm performs **depth** extrapolation in Fourier domain, the migration image is usually output in the depth domain. For migration-error correction, the depth-domain migrated common-offset sections were converted into PS two-way zero-offset time domain using the average of the one-way P-wave velocity and one-way S-wave velocity used for the migration process. Figures 8 and 9 are all shown in PS two-way zero-offset time.

In Figure 9, in the time window between 1400 and 1600 ms, the images from negative-offset sections (left half of each gather) are significantly different from the images from positive-offset sections (right half of each gather). Also, the event right below 2400 ms corresponds to different velocity values at negative-offset side and the positive-offset side. The interpretation of these phenomena is still in research, however, they suggest that it is always necessary to migrate the negative-offset and positive-offset (opposite azimuth in 3D) data separately.

In terms of event-flattening on common-image gathers, the differences between the gathers shown in Figure 8 and the gathers shown in Figure 9 are obvious. It is expected that the stacked image directly from the migrated common-offset sections and the image obtained by stacking the inverse NMO and NMO re-corrected common-image gathers are quite different. Figure 10 shows a portion of directly stacked image, and Figure 11 shows the same portion of the image from INMO-NMO corrected gathers.

There is no significant difference between the two images, although better spatial consistency and vertical resolution can be recognised by detailed analysis.

CONCLUSIONS

An algorithm for migrating separated common-offset sections is presented. The current implementation of this algorithm is time consuming because of the integration over wavenumbers in the offset direction. This method has been applied to Blackfoot vertical and radial-component data. The results show that, not only does this method provide high quality images, it also provides opportunities for detailed data analysis and interpretation. As for converted-wave data, separated migrated offset sections also leave a chance to correct error caused by migration velocity inaccuracy. This is very useful because in practice, the required S-wave migration velocities are rarely known with desired accuracy.

FUTURE WORK

Due to the many advantages of migration from common-offset sections, it is important to find more efficient algorithms to compute the migration filters in our

algorithm. The stationary-phase approximation method for evaluation of the wavenumber integral is being investigated and hopefully a more efficient algorithm with satisfactory accuracy will be implemented.

Even with the results, lots of analysis can be done to extract more meaningful interpretation information.

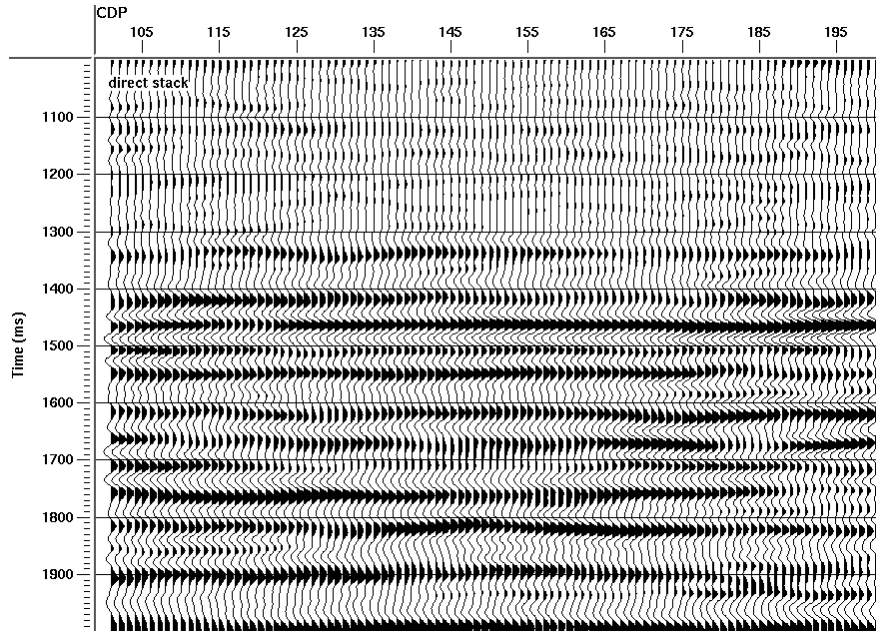


Figure 10: Radial component image by directly stacking the migrated common-offset sections

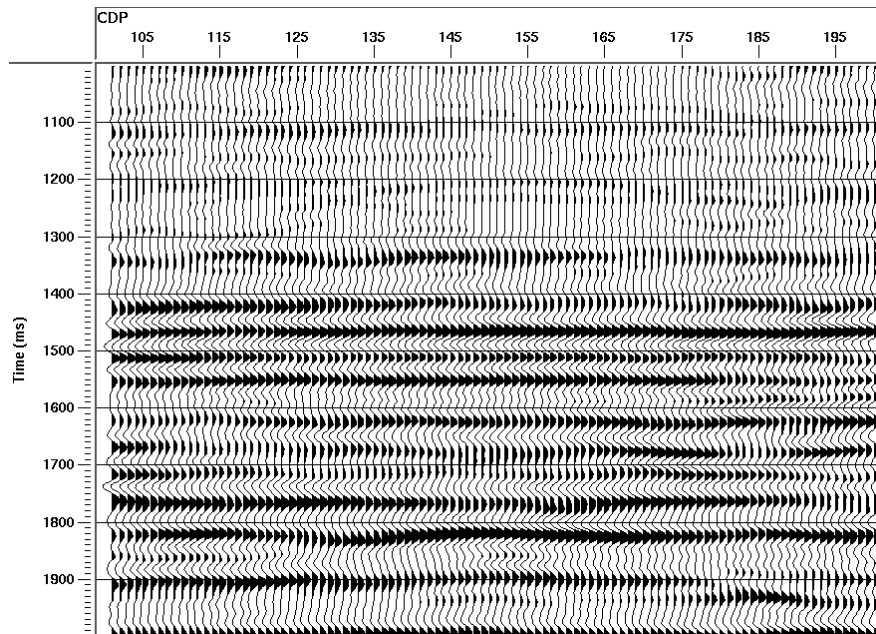


Figure 11: Radial-component image obtained from stacking the INMO-NMO corrected common-image gathers

ACKNOWLEDGEMENTS

The authors would like to thank the sponsors of the CREWES Project for their generous financial support. The discussions with Dr. Zhengsheng Yao have been very helpful. The help from Dr. Nanxun Dai of Varitas DGC, Calgary is appreciated.

REFERENCE

- Alkhalifah, Tariq, 1997, Prestack time migration for anisotropic media: 67th Annual Internat. Mtg., Soc. Expl. Geophys., Expanded Abstracts, 1583-1586.
- Dai and Marcoux, 1999, SEG Expanded Abstract.
- Deregowski, S. M., 1990, Common-offset migrations and velocity analysis: *First Break*, 8, no. 6, 224-234.
- Dubrule, A. A., 1983, Numerical methods for the migration of constant-offset sections in homogeneous and horizontally layered media: *Geophysics*, 48, no. 9, 1195-1203.
- Ekren, Bjorn O. and Ursin, Bjorn, 1995, Frequency-wavenumber constant-offset migration and AVO analysis: 65th Annual Internat. Mtg., Soc. Expl. Geophys., Expanded Abstracts, 1377-1380.
- Ekren, Bjorn O. and Ursin, Bjorn, 1999, True-amplitude frequency-wavenumber constant-offset migration: *Geophysics*, 64, 915-924.
- Ferber, R.-G., 1994, Migration to multiple offset and velocity analysis: *Geophys. Prosp.*, 42, no. 2, 99-112.
- Jin, Shengwen and Wu, Rushan, 1999, SEG Expanded Abstract.
- Kim, Young C. and Krebs, Jerry R., 1993, Pitfalls in velocity analysis using common-offset time migration: 63rd Annual Internat. Mtg., Soc. Expl. Geophys., Expanded Abstracts, 969-973.
- Li, X. and Margrave, G. F., 1998, Prestack $v(z)$ f-k migration for PP and PS data, CREWES Research Report, Vol. 10.
- Li, X. and Margrave, G. F., 1999a, Prestack $v(z)$ f-k migration for PP and PS seismic data, Expanded abstract, SEG annual meeting, Houston.
- Li, X. and Margrave, G. F., 1999b, On the computation of the offset wavenumber integral in phase-shift migration of common-offset sections, Research Report of CREWES Project, this volume.
- Li, X., Margrave, G. F. and Potter, C. C., 1999, $V(z)$ f-k Update, Research Report of CREWES Project, this volume.
- Margrave, G.F., 1998a, Theory of nonstationary linear filtering in the Fourier domain with application to time-variant filtering: *Geophysics*, 63, 244-259
- Margrave, G.F., 1998b, Direct Fourier migration for vertical velocity variations, Extended Abstracts, SEG meeting, New Orleans, USA.
- Margrave, G.F., 1998c, Direct Fourier migration for vertical velocity variations, The CREWES Project Research Report, Vol. 10.
- Mosher, C. C., Keho, T. H., Weglein, A. B. and Foster, D. J., 1996, The impact of migration on AVO: *Geophysics*, 61, no. 06, 1603-1615.
- Popovici, Alexander M., 1994, Reducing artifacts in prestack phase-shift migration of common-offset gathers: 64th Annual Internat. Mtg., Soc. Expl. Geophys., Expanded Abstracts, 684-687.
- Sattlegger, J. W., Stiller, P. K., Echterhoff, J. A. and Hentschke, M. K., 1980, Common offset plane migration (COPMIG): *Geophys. Prosp.*, 28, no. 6, 859-871.
- Tygel, M., Santos, L. T., Schleicher, J. and Hubral, P. 1999, Kirchhoff imaging as a tool for AVO/AVA analysis, *The Leading Edge*, August 1999, vol. 18, No. 8, 940-945.